Hydrogeology Journal
DOI 10.1007/s10040-014-1169-2

The freshwater lens of Benjamín Aceval, Chaco, Paraguay: a terrestrial analogue of an oceanic island lens

Georg Houben · Ursula Noell · Sara Vassolo · Christoph Grissemann · Mebus Geyh · Susanne Stadler · Eduardo J. Dose · Sofia Vera

Abstract The occurrence of a freshwater lens in the Paraguayan Chaco, 900 km away from the ocean, is reported. It is located underneath sandstone hills, surrounded by lowlands with predominantly saline groundwater. Its geometry was delineated using geoelectrical and electromagnetic investigations. The unusual height of the fresh groundwater level can be attributed to the presence of a confining layer at depth. The lens receives its recharge exclusively from rainfall during the hot and humid summer months. It predominantly contains water predating the atmospheric atomic bomb tests, some of it probably up to a thousand or more years old. The water balance shows that extraction currently does not exceed recharge in normal years. However, the available volume of groundwater leaves little room for a further increase of extraction in the future. Recharge is augmented by return flow from thousands of latrines and cess pits, and this has lead to widespread contamination of the groundwater by faecal bacteria.

Keywords Freshwater lens · Groundwater management · Water balance · Chaco · Paraguay

Received: 11 November 2013 / Accepted: 3 July 2014

Electronic supplementary material The online version of this article (doi:10.1007/s10040-014-1169-2) contains supplementary material, which is available to authorized users.

G. Houben (✉) · U. Noell · S. Vassolo · C. Grissemann · S. Stadler
Bundesanstalt für Geowissenschaften und Rohstoffe (BGR), Stilleweg 2, 30655, Hannover, Germany
e-mail: georg.houben@bgr.de

M. Geyh
Rübeland 12 - OT Bannetze, 29308, Winsen, Aller, Germany

E. J. Dose · S. Vera
Secretaria de Medio Ambiente (SEAM), Avenida Madame Lynch 3500, Asuncion, Paraguay

Published online: 24 July 2014

Introduction

The district and the town of Benjamín Aceval are located in the lower Chaco Boreal region, 35 km north of Paraguay's capital Asunción (Fig. 1). The Chaco is a sedimentary basin between the Andes to the west and the Rio Paraguay to the east, characterized by a very flat morphology. Even in the sub-humid eastern Chaco, where the study area is located, fresh water is scarce and groundwater mostly saline. The population density of the Chaco is accordingly very low. With roughly 247,000 km^2, it comprises 60 % of the land surface of Paraguay but hosts less than 2 % of its population (135,000 people). The city of Benjamín Aceval (including the villages Cerrito and Isla Ita), founded 1859, is a notable exception. Its population of about 17,000 is located on some isolated hills rising up to 25 m above the surrounding Chaco plain. Settlement was only possible due to the occurrence of fresh groundwater underneath these hills. Land use, except from the urban zone, is mostly dedicated to sugar cane plantations and cattle farming.

Practically nothing about the groundwater resource of Benjamín Aceval was known prior to this study. Overexploitation of freshwater and subsequent intrusion of saline groundwater from the adjacent lowlands was feared. Therefore, in the framework of the Paraguayan-German project PAS-PY (Protection and sustainable management of groundwater in Paraguay) a comprehensive hydrogeophysical exploration was performed whose aims were to delineate the freshwater aquifer and to deduce a water balance. This information is imperative to develop a sustainable water management concept for this fragile and irreplaceable water resource. Water quality issues were also addressed, as the city lacks a sewage collection and treatment system.

The interaction of fresh and saline water in coastal zones and oceanic islands has been studied in much detail (e.g. Cooper et al. 1964; Fetter 1972; Vacher 1988; Bear et al. 2010; Werner et al. 2012). Inland or terrestrial freshwater lenses are far less common and are often fed by river water infiltration (Cartwright et al. 2010). The occurrence of freshwater in Benjamín Aceval, although being located 900 km away from the nearest ocean, is a

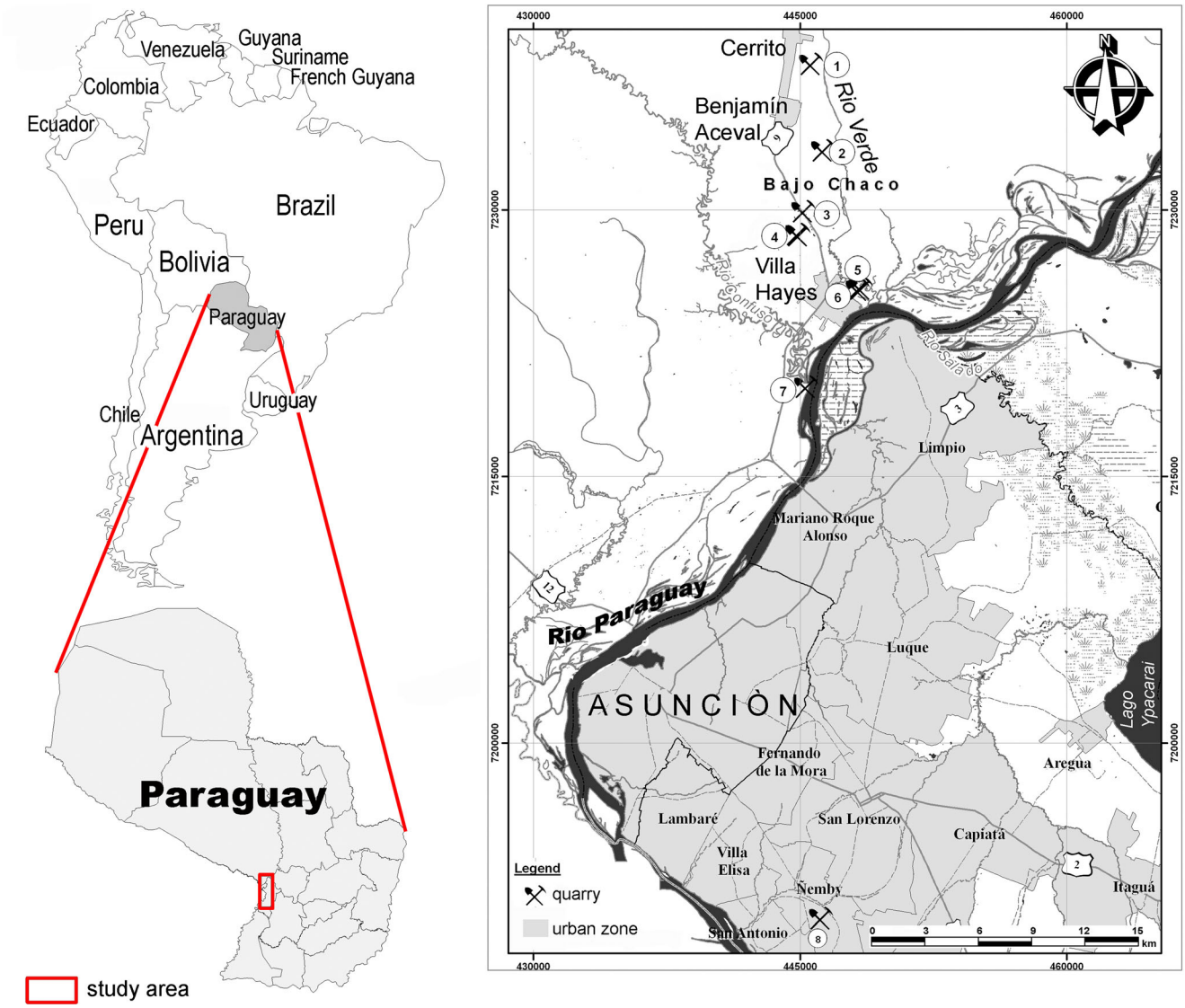

Fig. 1 Location map of the study area. Numbers indicate volcanic rock quarries: *1*ECOMIPA, *2*Kure Cua, *5–6*Cerro Verde, *7*Cerro Confuso, *8*Ñemby. Numbers for columnar sandstone: *3*Isla Ita, *4*Cerro Boli

terrestrial analogue of oceanic island freshwater lenses. In this case, the hills correspond to the island and the Chaco lowlands, with their predominantly saline groundwater, to the ocean.

Study area

Geology

The hills of Benjamín Aceval are comprised of a well-sorted, fluvial to aeolian reddish sandstone of weak cementation and relatively high porosity. The rock is petrographically very similar and probably identical to the Jurassic-Cretaceous Patiño Formation underlying Asunción on the other side of the Rio Paraguay; although, no final proof for this is available due to a lack of dateable fossils. The porosity of the Patiño sandstone, according to the analysis of some samples, is 10 %, a value also used in the following for this study site. Tropical weathering has caused the formation of a cover of several meters of loose sand and red clay. According to personal communication with drillers, the base of the aquifer is formed by a claystone layer at a depth of around 90–100 m. In two of the drillings, which reached this depth, such a layer is documented. No wells deeper than 100 m are available.

The area around Asunción and the lower Chaco contains some isolated volcanic intrusions which are or were mined in several quarries (Fig. 1). The intrusions are mostly circular and have diameters of up to several hundreds of meters although small dikes, which belong to the Asunción Alkaline Province (AAP), a series of undersaturated, mostly nephelinitic to phonolitic intrusions which are associated with the NW–SE oriented Asunción rift system, also occur (Bitschene 1987; Bitschene and Báez Presser 1989; Comin-Chiaramonti et al. 1991, 1997, 1999, 2007; Riccomini et al. 2001;

DOI 10.1007/s10040-014-1169-2

Velazquez et al. 2006). According to Bitschene (1987) they intruded during the early Tertiary (≈55–60 Ma). Previous geochemical and mineralogical analyses by the authors (Houben, Bundesanstalt für Geowissenschaften und Rohstoffe (BGR), unpublished data, 2014) revealed that the "basalts" of the two quarries in Benjamín Aceval are basanites, containing pyroxenes, nepheline, analcime and some olivine. During a geomagnetic survey, several so-far unknown intrusions were found, some larger, some just small dikes, all of them not visible at the surface. It was possible to distinguish two generations, one with normal, one with reverse magnetisation.

The volcanic intrusions have locally caused intensive contact metamorphism of the sandstones. The higher resistivity to erosion of both the volcanic intrusions and the contact metamorphites is probably the explanation for why the hills of Benjamín Aceval have not been eroded, as have the surrounding sandstones. Closest to the intrusions, the sandstone is completely recrystallized (quartzite) and bleached and porosity is as low as 2 %. Between the unaltered sandstone and the quartzite one can find a peculiar columnar sandstone which was mined for cobblestones. The prismatic columns have diameters of several centimetres and are often pentagonal or hexagonal, resembling basalt columns. Along the joints, the columnar sandstone is often bleached and its unusually high porosity of up to 40 % gives further evidence of strong dissolution processes. This rather unusual jointing was probably caused by shrinking during the cooling of the metamorphosed sandstone (Cortelezzi et al. 1988; Velázquez et al. 2008).

Climate

No meteorological station is available in Benjamín Aceval but the station of Asunción's airport in Luque is only 28 km to the south. Data covering the period 1971–2000 were available. The average annual air temperature is 23 ° C but shows a distinct annual variation (Fig. 2a). The average annual rainfall amounts to 1,400 mm/year, while potential evapotranspiration, calculated after Ivanov (1954), is 1,000 mm/year. The highest rainfall rates occur during the hot and humid summer months (Fig. 2b). In the short winter season, potential evapotranspiration exceeds precipitation (Fig. 2c,d); thus, any groundwater recharge should therefore take place in summer. The hilly landscape leads to significant and rapid surface run-off after the torrential summer rains.

Methods

The porosity of rock samples was investigated using a Micromeritics GeoPyc 1360 (Driflo). The geoelectric direct current measurements used the multi-electrode instrumentation GEOTOM (Geolog GmbH, Germany) which allows one to visually control the data quality during the measurement by observing the pseudo-sections. For the two-dimensional (2D) geoelectric profiles, the Wenner configuration with an electrode spacing of 4 m was used. Single profile length was 400 m (100 electrodes) and longer profiles were measured by overlapping several profiles. The inversion of the data into 2D resistivity sections was carried out with the finite difference software DC2DInvRES by Günther (2004).

For the time domain electromagnetic (TEM) soundings, a TEM-FAST 48HPC instrument (Applied Electromagnetic Research, USA) was used, including the one-dimensional (1D) inversion software TEM-Researcher provided by the same manufacturer. Transmitter loop sizes were usually 25 m × 25 m or 50 m × 50 m, when local conditions permitted, and a single loop configuration was used.

Water level fluctuations were measured at an hourly interval using a Level Troll 100 by InSitu Inc. (USA). The device measured absolute pressure, which was later corrected using atmospheric pressures recorded with an InSitu Baro Troll. Flow of surface water was measured using an Ott ADC (Ott Hydrometrie GmbH, Germany) following the norm EN ISO 748 (2007).

Parameters like pH, electrical conductivity, temperature, redox potential and dissolved oxygen of water samples were measured in the field using a WTW 350i device (WTW GmbH) installed in a flow cell (UIT GmbH, Germany). Cation and trace element samples were filtered (0.45 μm) and stabilised in the field by addition of nitric acid (65 %, ultrapure, Merck). Cations were analysed using ICP-OES (Spectro Ciros CCD, Spectro, USA). Dissolved inorganic carbonate species were determined by automatic titration using a Schott Titroline alpha plus. Ion chromatography (Dionex ICS-3000, USA) was used to analyse the remaining anions.

The presence and number of colonies of coliform bacteria and *Escherichia coli* was analysed locally applying the Quanti Tray method by Idexx (USA), using the Colisure nutrient, Quanti-Tray 2000 matrixes and a Quanti-Tray sealer type 2X. Samples were incubated 24–48 h at 35 ° C.

Stable water isotopes (δD, $\delta^{18}O$) were analysed in the LIAG laboratory, Hannover, until April 2011. $\delta^{2}H$ was analyzed using a chromium reduction system at 800 °C (H/Device, Thermo Finnigan, USA), coupled to a Thermo Finnigan Delta XP isotope ratio mass spectrometer. $\delta^{18}O$ was analyzed using an automated equilibration unit (Gasbench 2, Thermo Finnigan) in continuous flow mode. After April 2011, a L2120-i Laser Cavity Ring-down by Picarro (USA) was used. In the first months, both methods were applied to assure comparability of results. All samples were measured at least in duplicates and the reported value is the mean value. All values are given in the standard delta notation in per mil (‰) vs. Vienna Standard Mean Ocean Water (VSMOW). External reproducibility—defined as standard deviation of a control standard

DOI 10.1007/s10040-014-1169-2

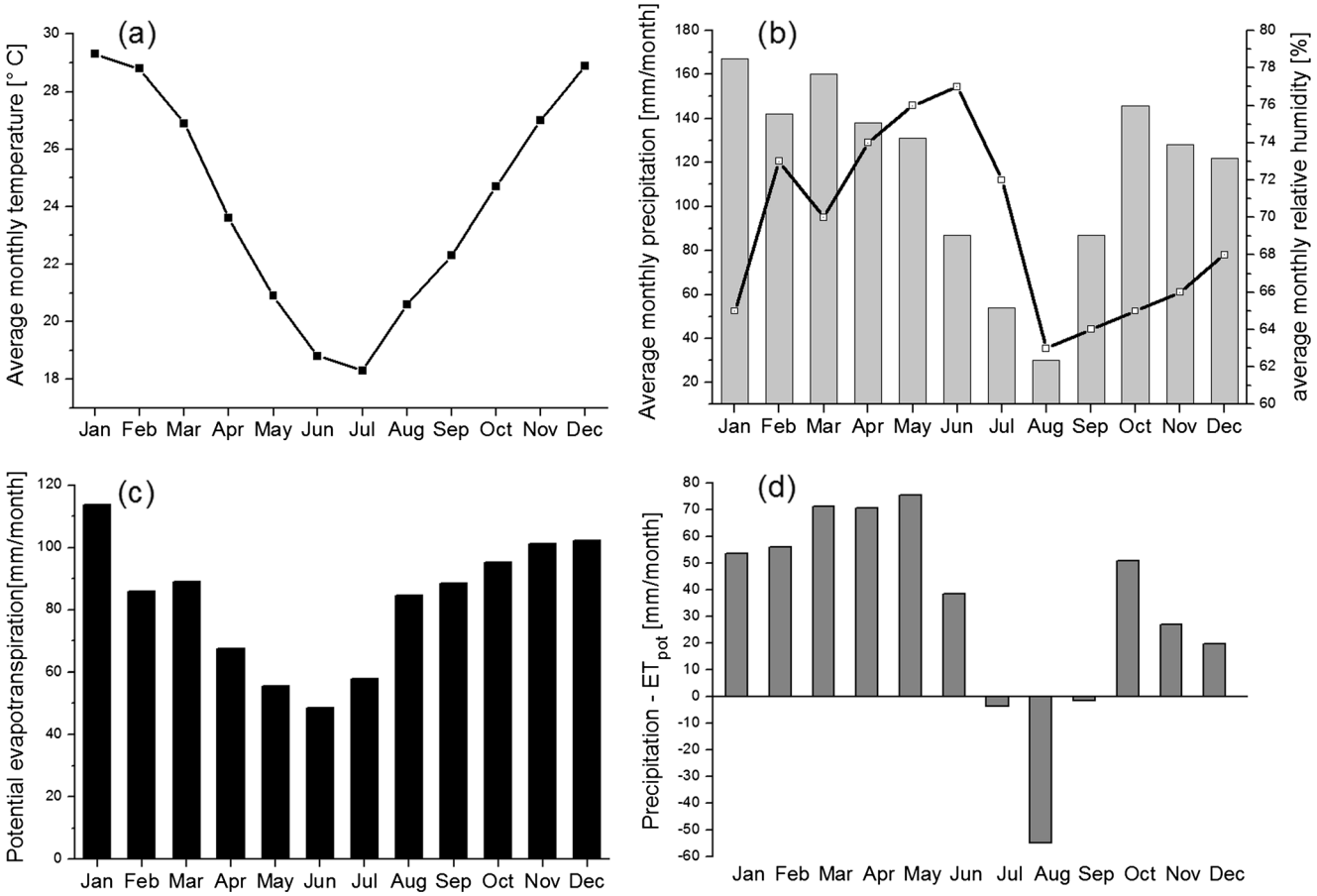

Fig. 2 **a** Temperature, **b** precipitation (*bars*) and relative humidity (*symbols*), **c** potential evapotranspiration calculated after Ivanov (1954), **d** difference between precipitation and potential evapotranspiration, after data recorded at the meteorological station of the Airport Asunción-Luque (1971–2000)

during all runs—was better than 0.8 and 0.2 ‰ for δD and $\delta^{18}O$, respectively.

Tritium was analysed at the Institute for Environmental Physics of the University of Bremen, Germany, using the tritium-ingrowth method after Clarke et al. (1976) on a mass spectrometer MAP 215–50 (Sültenfuß et al. 2009). The ^{3}H measurement precision is typically ±3 % and the detection limit is 0.02 tritium units (TU) for 500 g water (storage time 3 months).

The transient 2D cross-sectional model of the freshwater lens was set up using the numerical model code SEAWAT by the US Geological Survey (Langevin and Guo 2006). This code is based on MODFLOW/MT3DMS and allows for the calculation of density-driven flow processes. The model area was set to be a rectangle of 20,000 m width by 492 m depth, all initially saturated with saline water. Recharge at a rate of 80 mm/year was applied to a 3,700 m wide strip from the top of the model, representing the sandstone hills. Two drains were set at the left and right ends of the recharged strip to account for the springs emanating from the lens. Constant head boundary conditions were assumed to the left and right of the model. A hydraulic conductivity of $3 \cdot 10^{-6}$ m/s and a porosity of 10 % were used for the sandstone. The surface of the model beyond the sandstone hills was assumed to be covered by a sand layer with a hydraulic conductivity of $1 \cdot 10^{-6}$ m/s and a porosity of 15 %. A clay layer was located at a depth of 100 m. The densities of fresh and saline water were set to 1.000 and 1.025 g/cm^3, respectively.

Results and discussion

Geophysical exploration

The aim of the geoelectrical and electromagnetic investigations was to delineate the spatial limits of the freshwater lens (transition zone between fresh and saline water) and to assess its thickness, especially in its central part. The methodology included 2D direct current (DC) measurements along profiles and local 1D transient electromagnetic time domain (TEM) soundings. These two methods are the most useful for the type of exploration performed here (Barrett et al. 2002).

Due to the size of the investigation area, the geoelectrical profiles had to be located at strategic zones, without prior knowledge of the exact position of the transition zone. The profile length using 100

DOI 10.1007/s10040-014-1169-2

electrodes at a spacing of 4 m was 400 m, yielding a depth of information (DOI) of up to 60 m at the profile centre. However, the DOI depends not only on the resistivity of the subsurface but also on the noise conditions (Christiansen and Auken 2012) and 60 m are, therefore, a rough estimate. Sometimes, several profiles were linked, usually with an overlap of 100 m, resulting in profiles of up to 1,400 m length. In total 17.3 km of profiles were measured. Additionally, 53 TEM soundings were performed. The location of the profiles and the soundings is shown in Fig. 1 of the electronic supplementary material (ESM). An example of a geoelectrical profile is given here in Fig. 3. The TEM soundings indicated maximum freshwater thicknesses of 90–110 m. These were found, as expected, close to the highest morphological elevations, located between Benjamín Aceval and Cerrito.

The results of the geophysical exploration were combined with measurements of the electrical conductivity of groundwater in the wells, as well as morphological and geological constraints to delineate the borders of the freshwater body. The presence of Caranday palm trees (*Copernicia alba*, Arecaceae family) also proved to be a very good indicator of saline groundwater. There is one big lens, covering almost all of the city of Benjamín Aceval and the village Cerrito, and two smaller independent freshwater bodies to the south (see ESM). The lens geometry is mostly controlled by morphology.

Hydrogeology

As only two supply wells had observation wells close by, two pumping tests were performed, of 6 and 8 h duration. The observation borehole of the first test, situated 15 m from the pumping well, showed a small drawdown (0.5 m) compared to the assumed aquifer thickness (50 m) at a pumping rate of 6.6 m^3/h; therefore, the Cooper-Jacob time-drawdown method (Batu 1998) was used. The drawdown curve shows two slopes, probably corresponding to two types of porosity. The first can probably be attributed to fractures and yielded a transmissivity of $T=2.2 \cdot 10^{-3}$ m^2/s; the second, probably related to the intergranular matrix porosity, yielded a transmissivity of $T=1.2 \cdot 10^{-3}$ m^2/s. The recovery test gave similar results. The mean resulting hydraulic conductivity of $3 \cdot 10^{-5}$ m/s is in the upper range of typical values for sandstones (Spitz and Moreno 1996). This is reasonable considering its aeolian origin and weak cementation of the matrix. The well for the second pumping test is located close to a volcanic intrusion and the sandstone is thus more compact due to contact metamorphism. Even at low pumping rates of 1.4 m^3/h, high drawdowns of 25 m were observed in the well which negatively affected the quality of analysis. Drawdown in the observation well, situated 19 m away, was about 2 m. Obtained transmissivities range between $T=5 \cdot 10^{-6}$ and $T=4 \cdot 10^{-5}$ m^2/s, significantly lower than for the first test, but still in the range common for low-permeability sandstones (Spitz and Moreno 1996). The resulting hydraulic conductivity is about $7 \cdot 10^{-7}$ m/s. For all following calculations a mean hydraulic conductivity of $1 \cdot 10^{-6}$ m/s and a porosity of 10 % were used.

Equipotential maps were prepared for July 2009 and 2010. As the outcome was very similar for both years, only the 2009 map is presented here (Fig. 4). Measurements were taken in July because this is usually the coldest month in Paraguay with lowest water consumption. Active wells were turned off at least 8 h prior to measuring its water level. Due to technical reasons, not all wells could be turned off, so these were not measured. In some wells, the water level is not accessible as the wellhead is tightly closed. The scarcity of measured water levels did not allow

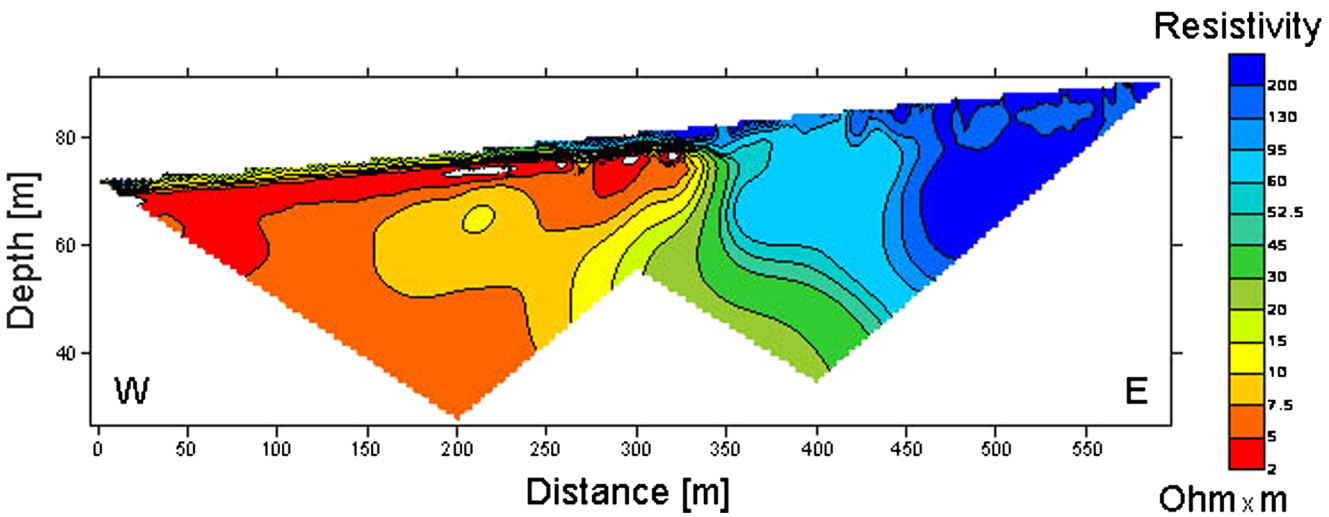

Fig. 3 Geoelectrical 2D profile (T13 in Fig. 1 of the ESM) showing distribution of electrical resistivities

DOI 10.1007/s10040-014-1169-2

the construction of an equipotential map for the southern part of the freshwater lens. The resulting map for the northern part, nevertheless, shows the classical pattern of a freshwater lens underneath a topographical elevation, delimited by surrounding saline water. Flow from the lens is directed towards the surrounding lowland. The exfiltration of freshwater from the lens at the foot of the hill is diffuse. Some small to very small springs occur along the rim of the lens, often only visible as wet soil zones.

According to a shallow test drill hole in the surrounding lowland, the saltwater level is at about 60 m above sea level (asl; 3 m below the surface). High gradients of the saline groundwater level are not probable considering the flat Chaco surface. The water encountered had a density of 1.025 g/cm^3, close to that of seawater. It cannot be ruled out that deeper groundwater might be even more saline as this is common in the central Chaco.

Even the lowest freshwater levels in the lens are higher than the river water levels of the adjacent Rio Verde; thus, outruling infiltration of river water as a source of groundwater recharge. The highest freshwater levels were found, as expected, in the zone with the highest ground level elevation, between Benjamín Aceval and Cerrito. With a groundwater level of 78.5 m asl, it is 18.5 m higher than the salt water level mentioned in the preceding.

Due to the fact that almost all wells are in use and the few inactive wells are very close to active ones, it was only possible to measure water level fluctuations in one well (Fig. 5), with a depth to groundwater of around 15–16 m, which is located at the border of the freshwater lens but is sufficiently far away from pumping wells. From the curve in Fig. 6, it can be inferred that:

1. The thick unsaturated zone levels out all short-term effects as there are no significant peaks visible which can be attributed to individual rainfall events.
2. The water level of the lens does not reflect the seasonal fluctuations of the water level of the Rio Verde or Rio Paraguay, the latter usually showing an amplitude of 2–5 m (McClain 2002).
3. The seasonal fluctuation of the groundwater level, hence, appears to be solely caused by infiltration (groundwater recharge) and subsequent exfiltration.

Groundwater levels start to rise in April or May and reach their maximum around October to November, i.e. after the end of the dry season. As the climate data showed, recharge during the dry season itself can be ruled out. Recharge occurs most probably during the hot and rainy summer season. As water levels reach their maximum in the dry season, a significant time lag between infiltration at the surface and arrival at the groundwater surface can be inferred. From our limited time period of measurements, it cannot be inferred that the rise visible in Fig. 5 is attributable to the preceding summer. Transit time in the unsaturated zone might take more than 1 year. Assuming that the measured rise of the water level of 1.4 m in 2009 was caused only by infiltration of rainwater, and considering a porosity of 10 %, groundwater recharge is estimated to be around 140 mm/year, equivalent to 10 % of annual rainfall.

The simplified chloride method was used to calculate groundwater recharge (Kinzelbach et al. 2002).

$$r = \frac{[\mathrm{Cl_{rain}}]}{[\mathrm{Cl_{groundwater}}]} \cdot P \qquad (1)$$

with

r	groundwater recharge rate [mm/year]
$[\mathrm{Cl_{rain}}]$	chloride concentration in rainwater [mg/l]
$[\mathrm{Cl_{groundwater}}]$	chloride concentration in groundwater [mg/l]
P	mean annual precipitation [mm/year]

Chloride concentrations in rainfall from Asunción were sampled eight times between 2008 and 2010. Concentrations vary between 0.06 and 0.20 mg/l. Chloride concentrations in groundwater show a large variation, as many wells are affected by wastewater infiltration. Taking into account only the few uncontaminated wells, that is, those not located in urban zones, concentrations of 2–3 mg/l, representative for natural recharge, were found. Using these values and the mean annual precipitation of 1,400 mm/year, Eq. (1) yields recharge rates between 30 and 140 mm/year, with an arithmetic mean of 85 mm/year. Since no data on surface run-off were available, no corrections for its influence could be considered.

The role of the Rio Verde for the water balance of the freshwater lens had to be investigated as it flows immediately along the eastern border of the hill chain of Benjamín Aceval and the freshwater lens. The river has a huge catchment to the north of the study area and responds quickly to rainfall events there. Two bridges where the river is diked and flow is focused to constructed outlets, one in the north, one in the south (for location, see ESM), were selected. The difference between both measurements should give insight into volumes of water moving from the lens to the river and vice versa. In the first year of flow measurement, rather than an increase, a decrease of flow rates from north to south was found, which cannot be attributed to infiltration towards the lens because, as already discussed, the heads there are several metres higher than in the

DOI 10.1007/s10040-014-1169-2

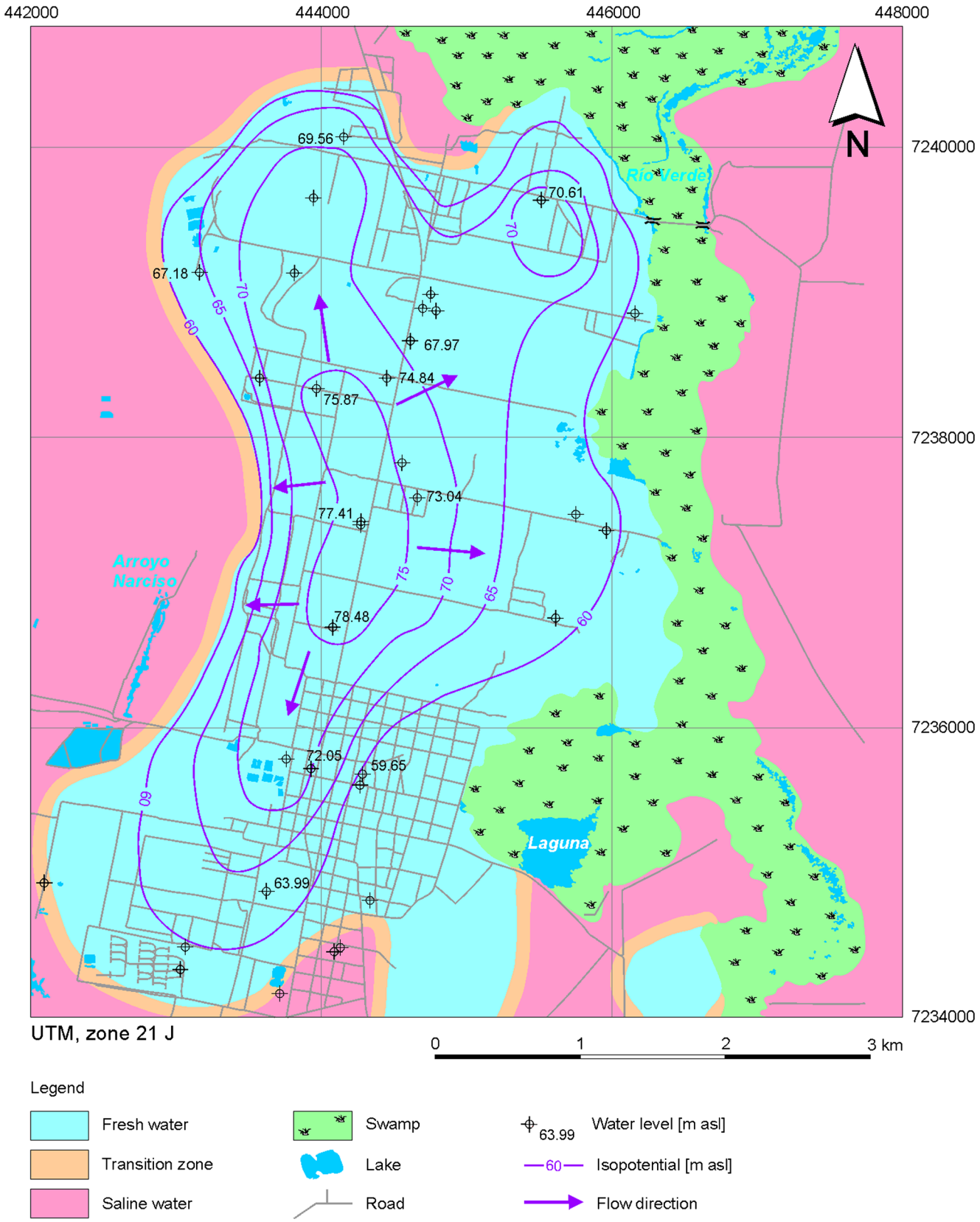

Fig. 4 Equipotential map of the northern part of the freshwater lens (Benjamín Aceval - Cerrito), July 2009

river (Fig. 4). The decrease in discharge is caused by evaporation from open water surfaces and transpiration by abundant water plants such as Piri (*Scirpus californicus*, Ciperaceae family) which are

DOI 10.1007/s10040-014-1169-2

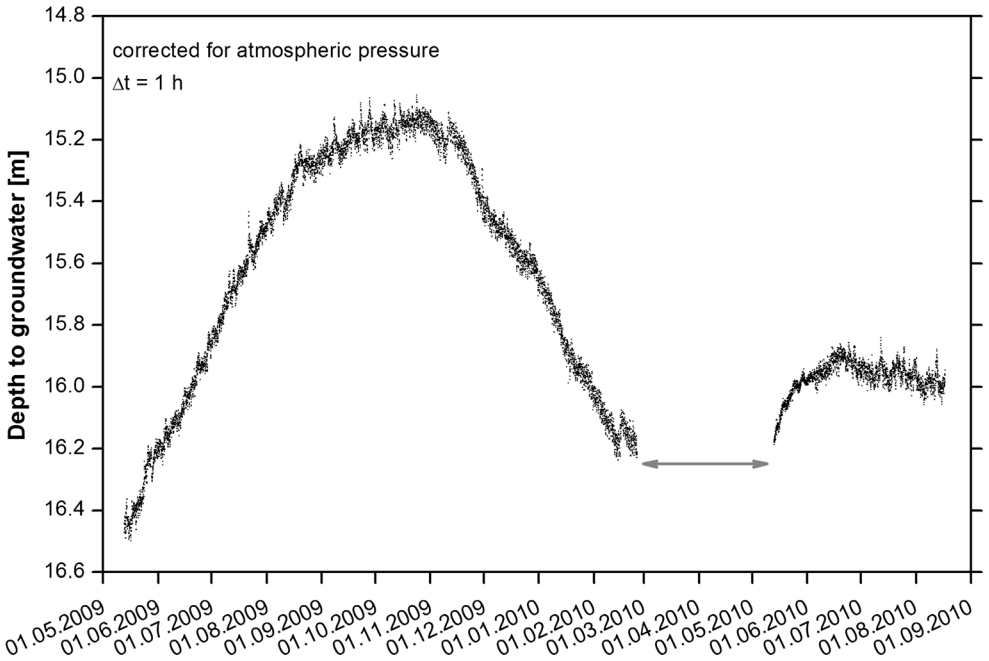

Fig. 5 Water level fluctuations in the inactive Mendieta well (date format DD.MM.YYYY). The *arrow* indicates data loss due to a malfunction of the logger

found in the vast swamp area the river has to cross between the two bridges. This consumes so much water that any infiltration of groundwater into the river is less than the uncertainty in the measurements. If no rain occurs in the upper catchment, sometimes flow in the Rio Verde ceases completely. From this, it can be concluded that the groundwater volume flowing into the river from the eastern rim of the freshwater lens must be rather small, as it cannot maintain even a small base flow.

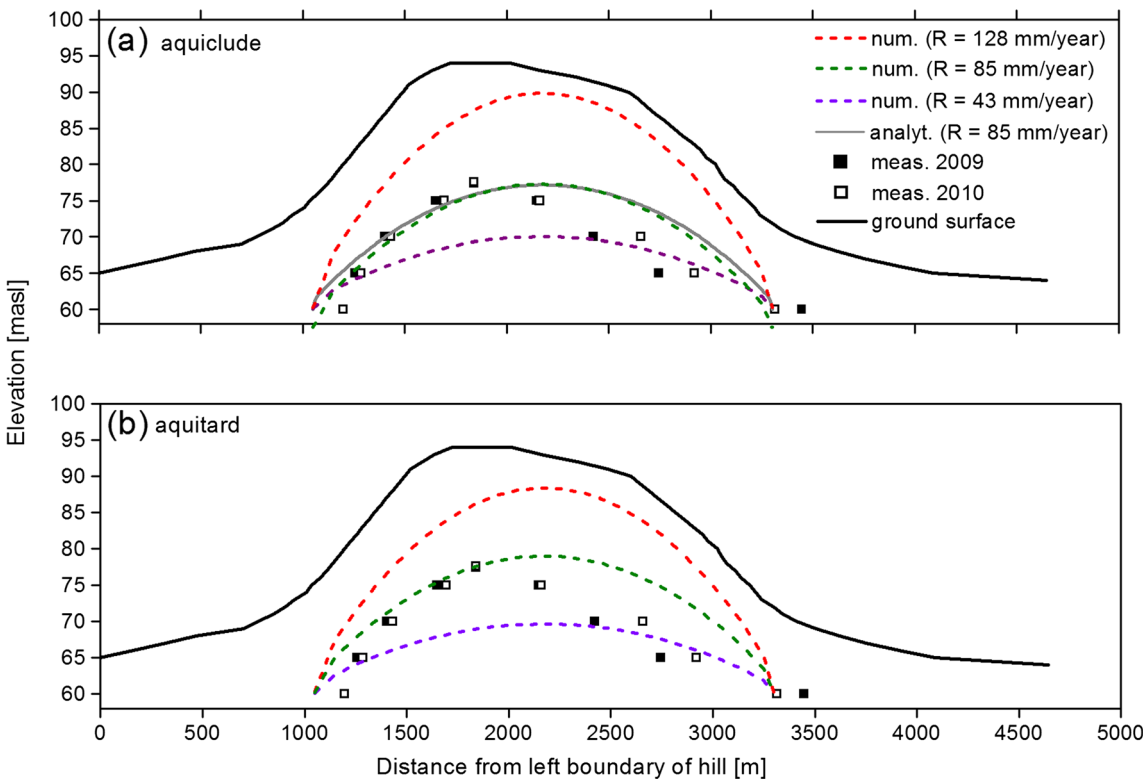

Fig. 6 Comparison of measured elevations of the fresh groundwater surface to numerical models with different recharge rates and an analytical model for a *truncated lens* (Vacher 1988), assuming the presence of **a** an aquiclude and **b** an aquitard

 DOI 10.1007/s10040-014-1169-2

Modelling of the freshwater lens

Given the morphological situation, the freshwater lens could have developed according to the classic Ghyben-Herzberg model (Baydon-Ghyben 1898; Herzberg 1901) with low-density freshwater floating on top of the denser saline water. Given the elongated lens shape described above, it may be approximated mathematically as an infinite-strip island (Fetter 1972; Vacher 1988).

According to the Ghyben-Herzberg Eqs. (2) and (3), the depth extent of the lens can be estimated by the formula

$$z = h \times \alpha \tag{2}$$

$$\alpha = \rho_f/(\rho_s - \rho_f) \tag{3}$$

with

- z depth of the interface below sea level [m]
- h height of the fresh groundwater level above the salt-water level [m]
  Ghyben-Herzberg density ratio [−]
- ρ_f density of freshwater
- ρ_s density of saltwater

With densities for freshwater and seawater of 1.000 and 1.025 g/cm^3, respectively, α equals 40. Applying Eq. (2) to the freshwater lens of Benjamin Aceval, it would thus have depth to interface of around 680 m at a measured h=17 m. Such a thick lens is not realistic, considering the maximum thickness of the Patiño Formation of 300 m. Additionally, the TEM soundings indicated maximum freshwater thicknesses of 90–110 m. Our lens obviously shows two anomalies, too large height of the freshwater level (h) and too small depth to interface (z). Such a deviation from the "standard" geometry of a freshwater lens may occur when the lens is truncated at depth by an impermeable deeper layer which inhibits further vertical propagation of freshwater (Ayers and Vacher 1986; Vacher 1988; Bailey et al. 2009; Dose et al. 2014). As mentioned in the preceding, impermeable claystone intercalations at around 100 m depth are documented in drilling logs from the investigation area.

The height of the freshwater level in a truncated lens can be calculated using Eqs. (4) and (5) after finding h_b and x_1 from Eqs. (5) and (6) (Vacher 1988; Dose et al. 2014). Equations (5) and (7) have to be solved iteratively. The height of the freshwater level has to be calculated for two sectors, one for the sector where h is not limited by the impermeable layer (h_I, Eq. 4), and one for the truncated inner part (h_{II}, Eq. 5). The boundary between both sectors at x_1 is the refraction point. The total thickness of the lens (or the interface depth) can be calculated using Eq. (2).

$$h_1^2 = \left[\frac{R}{K(\alpha+1)}\right]\left(Lx - c^2\right) \tag{4}$$

$$K\left(h_{11}^2 - h_b^2\right) + 2KB_1(h_{11} - h_b) = R\left[L(x - x_1) - \left(x^2 - x_1^2\right)\right] \tag{5}$$

$$h_b^2 = \left[\frac{R}{K_1(\alpha+1)}\right]\left(Lx_1 - x_1^2\right) \tag{6}$$

$$2Mx_I - x_I^2 = \frac{\left[K_1(\alpha+1)B_I^z\right]}{R\alpha^z} \tag{7}$$

with (see also Fig. 6):

- $h_{I,II}$ height of freshwater level above saline water level in sectors I and II [m]
- h_b fresh groundwater level at the interface refraction [m]
- R recharge [m/s]
- K hydraulic conductivity [m/s]
- x horizontal coordinate, distance from "shore"[m]
- x_1 horizontal coordinate of refraction point [m]
- L width of the cross-section along x axis [m], here 2,250 m
- Z thickness of the aquifer layer below sea level [m]

The application of this model showed that, at a recharge rate of R=85 mm/year and a mean hydraulic conductivity of $K = 1 \cdot 10^{-6}$ m/s, the maximum fresh groundwater level reaches almost 15 m above the saltwater level and, thus, is similar to the field observations (Fig. 6). With significantly smaller recharge values, the interface does not reach down to the impermeable layer. Higher recharge rates lead to excessive freshwater heads (overflow). The model cannot, however, address the geometrical asymmetry of the lens and, therefore, the highest elevations of the freshwater surface to the west of the lens was focused on in this study.

The case of the truncated symmetric freshwater lens was also modeled numerically. The main motivation of this was to study the influence of the aquitard and to test whether its inferred existence can be confirmed. As such, it serves as a test of the conceptual model whose area was a rectangle of 20,000 m width by 492 m height, all initially saturated with saline water. Recharge at a rate of 85 mm/year was applied to a 2,250-m-wide strip in the

DOI 10.1007/s10040-014-1169-2

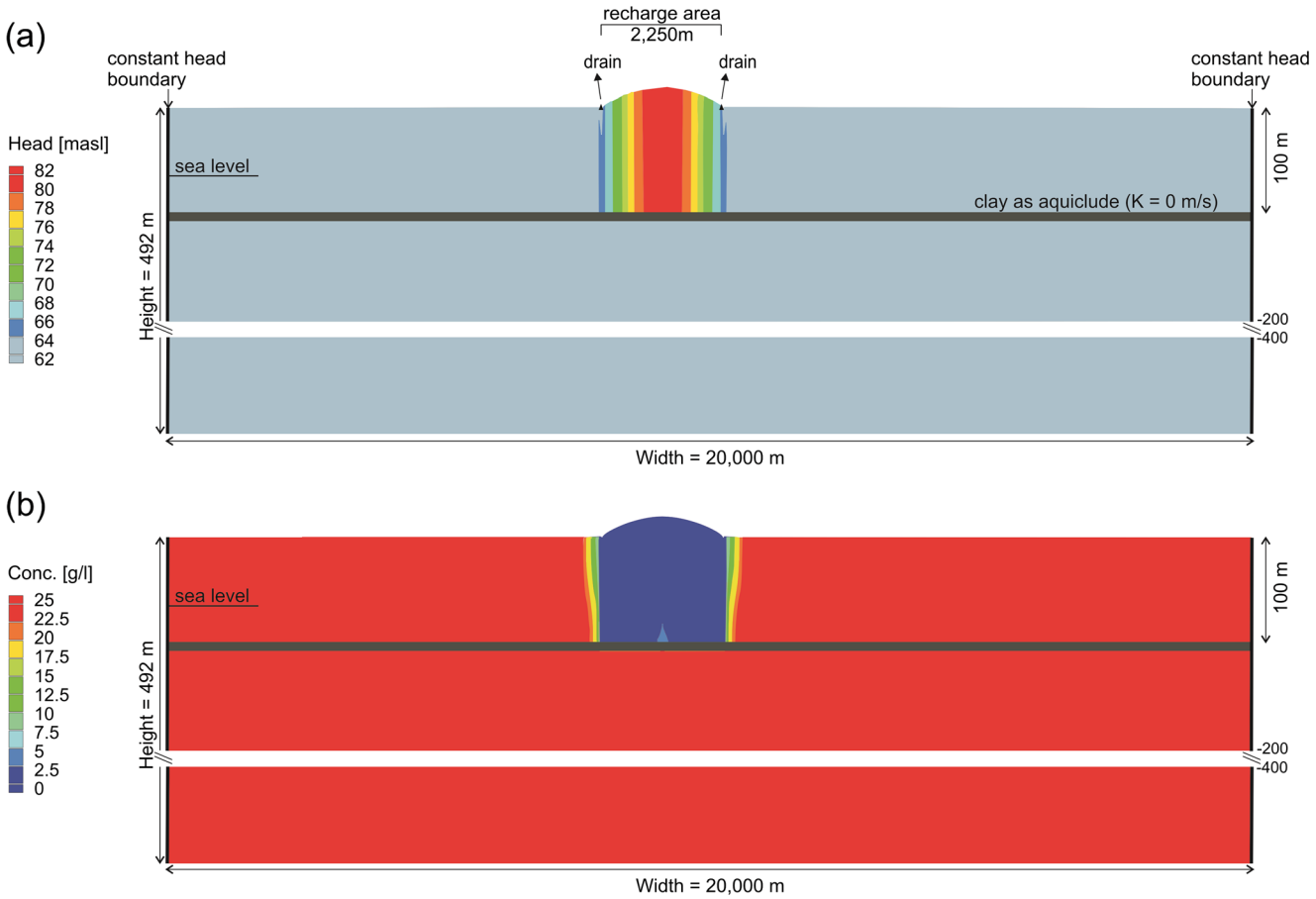

Fig. 7 Numerical simulation of **a** head and **b** concentration distributions for an aquiclude located at 100 m depth. After 500 years, the maximum fresh groundwater level reaches 17 m in height and almost the entire lens consists of freshwater

middle of the model, representing the sandstone hills rising from the Chaco plain. Two drains were set at the left and right ends of the recharged strip to account for the springs emanating from the lens. Constant head boundary conditions were assumed to the left and right of the model. A horizontal hydraulic conductivity of $1 \cdot 10^{-6}$ m/s and a porosity of 0.10 were used for the sandstone. The surface of the model beyond the sandstone hills was assumed to be covered by a sand layer with a hydraulic conductivity of $1 \cdot 10^{-8}$ m/s and a porosity of 0.15. A low-conductivity layer (clay) was placed at a depth of 100 m. The vertical hydraulic conductivities were assumed to be equal to the horizontal. Densities of fresh and saline water were 1.000 and 1.025 g/cm^3, respectively.

In a first approach, the clay layer at 100 m depth was considered as impermeable (K=0 m/s). After 500 years, the freshwater lens reaches steady-state heads and salt concentrations (Fig. 7). The resulting maximum fresh groundwater level of 17 m above the saltwater level coincides well with the field observations (equipotential map) and the analytical model (Fig. 6).

In a second approach, the clay layer was modelled as an aquitard (K=$1 \cdot 10^{-10}$ m/s, n=0.15), which would allow freshwater to proceed further downwards. Results for this case (Fig. 8) show that the freshwater lens formation requires more time. After 500 years, steady state has been reached for the hydraulic heads but not yet for the salt concentration. The resulting maximum height of the fresh groundwater level at 16 m (Fig. 9) is also similar to the field observations and analytical model. After the simulation period of 500 years, the concentration below the aquitard would still be in the range of brackish water.

Which of the two approaches is more close to reality cannot be decided at this stage because there are no measurements of salt concentrations below the clay layer and the used geophysical methods cannot penetrate to these depths. To analyse the effect of the recharge rate, further numerical calculations were performed for both cases, considering recharges of 50 % above and 50 % below the value of 85 mm/year (128 and 43 mm/year, respectively). The higher recharge leads to maximum fresh groundwater level of 27 or 25 m for the aquiclude and aquitard cases, respectively (Fig. 6). For the lower recharge, maximum groundwater level reaches 7 m for the aquiclude case and 6 m for the aquitard. These tests show that a recharge rate of 85 mm/year is the most probable.

Isotope studies

The stable water isotopes ^{18}O and ^{2}H and the radioactive isotope ^{3}H were studied to investigate the interrelation of

DOI 10.1007/s10040-014-1169-2

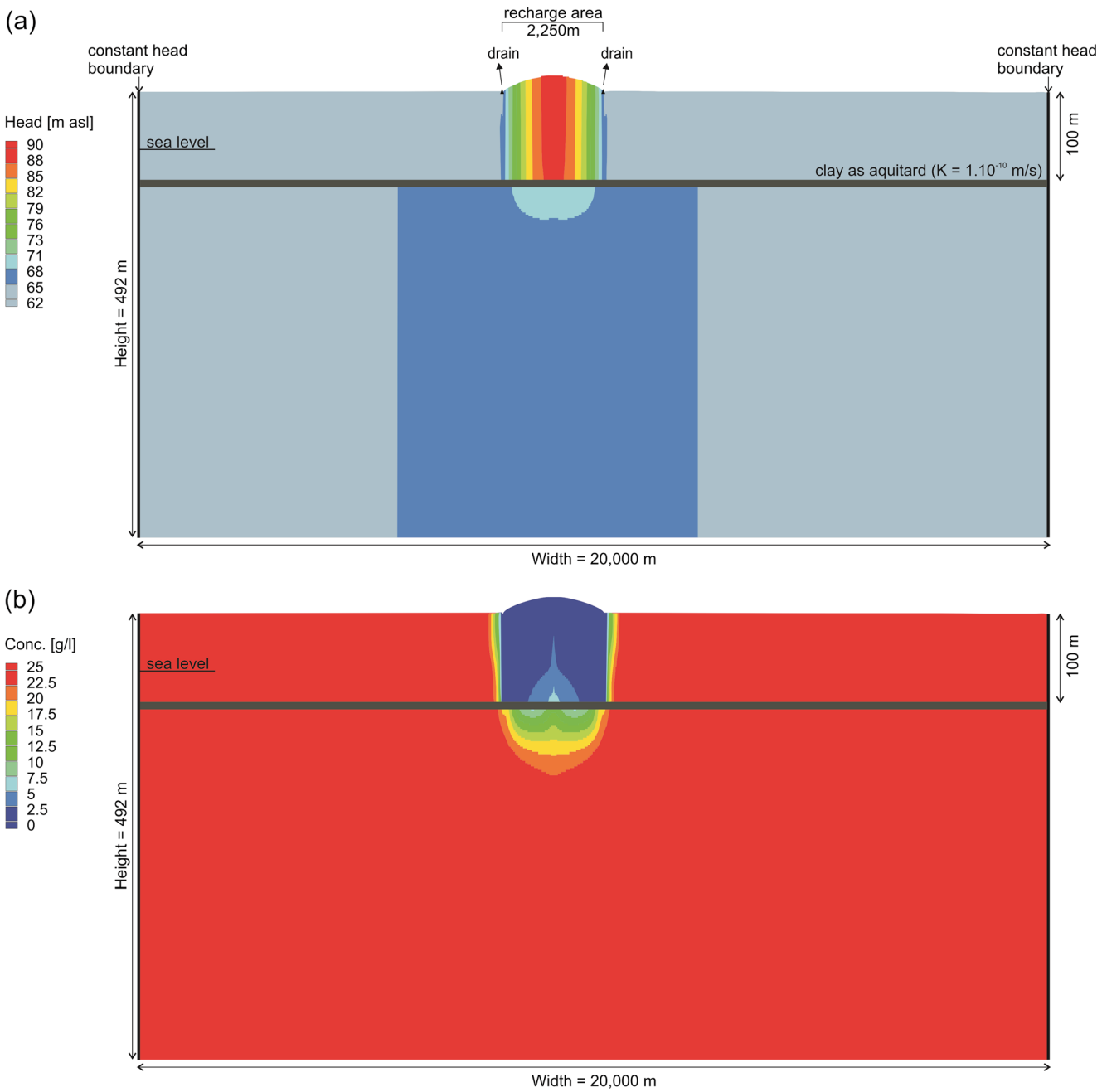

Fig. 8 Numerical simulation of **a** head and **b** concentration distributions for an aquitard at 100 m depth. After 500 years, the maximum fresh groundwater level reaches 16 m in height and concentrations of 40 % of the initial salinity below the aquitard

rainwater, groundwater and river water. Stable isotopes were analysed for the Rio Verde (26 samples), all 38 water wells and 89 rainwater samples, the latter taken between October 2008 and July 2012 in Asunción-Luque. Historic data of the isotopic composition of rainwater from Paraguay are scarce. The global network of isotopes in precipitation (GNIP) by the International Atomic Energy Agency (IAEA) only provides a few $\delta^{18}O$ and $\delta^{2}H$ data from the 1960s for station 8621700 (Asunción). Additionally, a few $\delta^{18}O$, $\delta^{2}H$ and ^{3}H data by Facetti-Fernandez and Stichler (1995) collected between 1993 and 1994 throughout Paraguay were available. Other stations in Brazil and Argentina are located too far away and have different climate.

Figure 9 shows a plot of all available $\delta^{18}O$ and $\delta^{2}H$ values for rainwater. The samples taken during this study plot along a local meteoric water line (LMWL) described by $\delta^{2}H=7.9\ \delta^{18}O+8.8$. The GNIP values, which are some 40 years older, also plot along this LMWL, as do the samples taken by Facetti-Fernandez and Stichler (1995) in the early 1990s. Therefore, it was assumed that the stable isotope composition of the precipitation around Asunción has remained constant at least in the last 50 years and probably before.

DOI 10.1007/s10040-014-1169-2

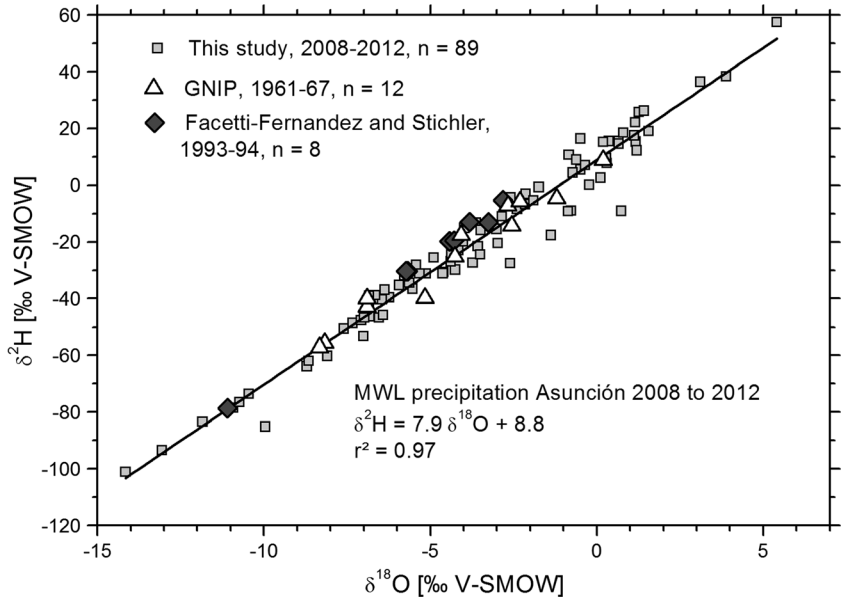

Fig. 9 $\delta^{18}O$ and $\delta^{2}H$ of rainwater samples from this study (2008–2012), GNIP data (1961–1967) and Facetti-Fernandez and Stichler (1995). The meteoric water line (*MWL*) shown is based only on the data from this study. The samples from this study and GNIP were taken in Asunción, the ones by Facetti-Fernandez and Stichler (1995) in several locations in eastern Paraguay

Figure 10 compares the seasonal variation of $\delta^{2}H$ over the course of the year for the GNIP data, some data by Facetti-Fernandez and Stichler (1995) and our own samples. All show a periodic pattern with markedly more positive values of $\delta^{2}H$ during the relatively dry and cold months. The curves coincide well in the humid months from September to May. The deviation visible during the dry months from June to August should not be over-interpreted, though. Rainfall is infrequent in this period, mostly some short events of low intensity. It was only possible to collect three samples in August and four in September between 2008 and 2012. It should also be noted that our values are not weighted, as no daily precipitation data were available. The annual variation for $\delta^{18}O$ shows the same behaviour (not shown here). In addition, Facetti-Fernandez and Stichler (1995) and our data both do not show the light value recorded for August as seen in the GNIP data. It was assumed that the seasonal pattern has been valid through the late Holocene. As the climatic conditions during the winter do not allow for groundwater recharge due to a negative water balance (Fig. 2), recharged water from the humid period should show light $\delta^{18}O$ and $\delta^{2}H$.

The stable isotopes of the groundwater samples plot between −7.0 and −4.5 ‰ for $\delta^{18}O$ and −45 and −25 ‰ for $\delta^{2}H$ (Fig. 11); thus, they cover a range typical for rainwater from average wet season conditions (November–April) where climatic conditions indeed favour groundwater recharge (Fig. 10). The spread of the rainwater samples around the MWL covers the groundwater samples so that one could assume that both have a common origin; however, almost all groundwater samples

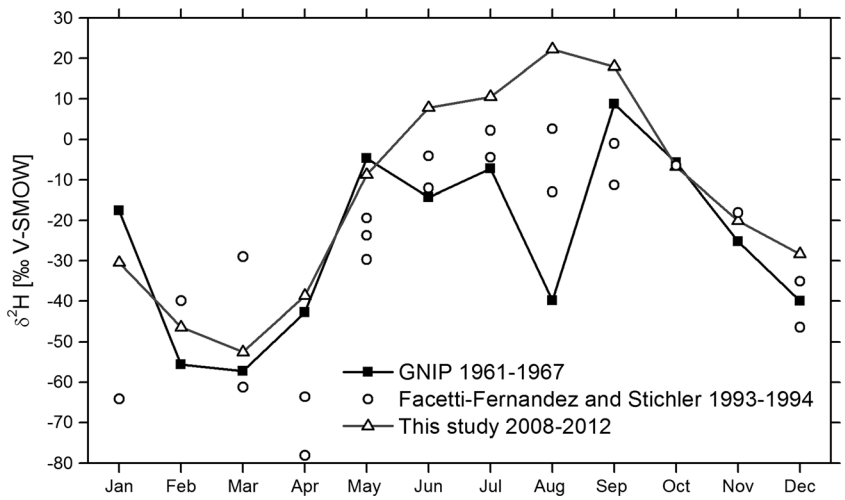

Fig. 10 Seasonal variation of mean monthly $\delta^{2}H$ of rainwater from Asunción, 1961–1967 (*GNIP*), 1993–1994 (Facetti-Fernandez and Stichler 1995) and own data from 2008 to 2012

 DOI 10.1007/s10040-014-1169-2

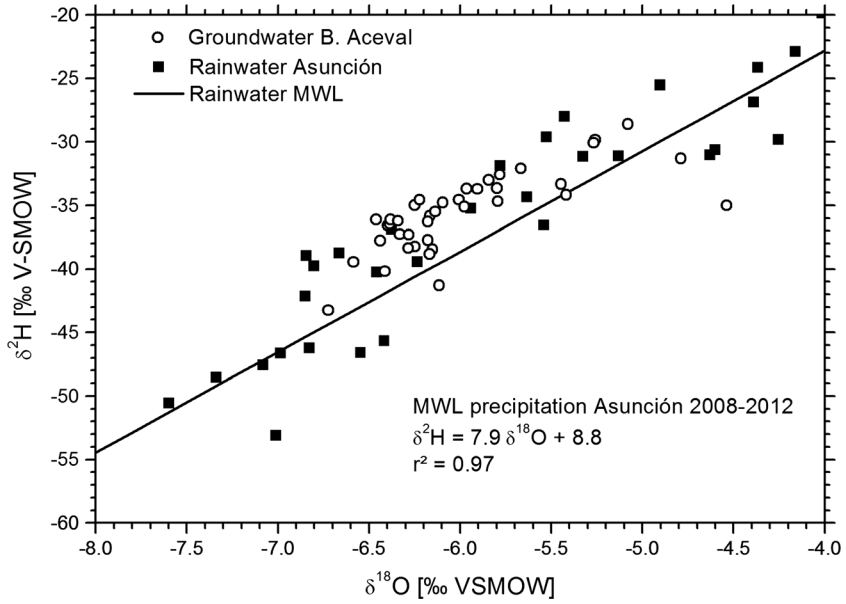

Fig. 11 $\delta^{18}O$ and $\delta^{2}H$ of groundwater from Benjamín Aceval compared to recent rainwater from Asunción (see Figs. 9 and 10)

plot above the meteoric water line with a mean deuterium offset of around 12.0 ‰, instead of 8.8‰ for the LMWL, which is a difference larger than the analytical standard deviation. Such a deviation "to the left" from the MWL cannot be attributed to water–rock interactions or evaporation. One possible explanation would be that this groundwater was recharged during a time with different climate and isotopic composition of rainwater, e.g. the humid Tauca phase which occurred in South America 13,000–8,500 years before present (Veit 1995; Geyh et al. 1999; Grosjean and Veit 2005). On the other hand, the mean deuterium offset of 8.8‰ might be biased by the most and least depleted samples which are not reflected in the isotopic signatures of the groundwater (Fig. 11). Neglecting those would shift the MWL towards higher offsets, indicating that the groundwater was formed under a similar climate as today. This is in good agreement with maximum groundwater travel times of up to 3,500 years calculated applying the analytical model by Chesnaux and Allen (2008), Fig. 12). The age stratification was also calculated according to the analytical model developed by Greskowiak et al. (2013) which yielded maximum ages of around 1,000 years. These results comply with the numerical model which predicts travel times in the same range.

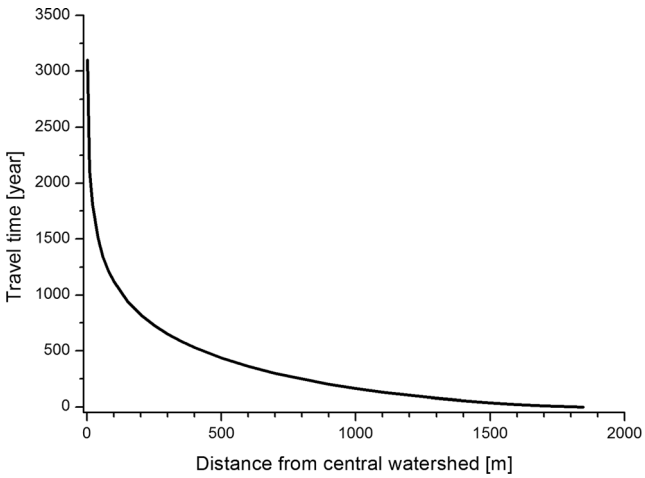

Fig. 12 Travel times of groundwater in the Benjamín Aceval freshwater lens calculated after Chesnaux and Allen (2008). The origin of the x axis is the highest freshwater height, that is, the centre of the lens

Six rainwater samples taken between 2009 and 2010 yielded tritium concentrations ranging between 2.43 and 3.03 TU, calculated for 1 January 2010, with a mean of 2.67 TU. In all, 18 groundwater samples were analyzed for their tritium value, which ranged from 0.01 to 0.56 TU, indicating the presence of "young" (post-bomb) water in the lens. Its percentage cannot be calculated due to the lack of a reliable input curve and the unknown depth of pump and screens. The bulk of the water, nevertheless, is tritium-free and must, therefore, predate the atmospheric bomb tests.

Freshwater lenses usually show a vertically stratified distribution of groundwater ages (Stoeckl and Houben 2012). During a recharge event, here the humid period, a layer with a discrete age is recharged to the top of the water column. The thickness of this layer depends on the recharge rate which is controlled by the climatic conditions. During the next recharge phase, the previous layer will be displaced downwards. Age layers become successively thinner with time due to ongoing exfiltration at the sides. Age thus increases exponentially with depth (Vogel 1967, 1970; Greskowiak et al. 2013). The lens studied here probably is very similar, as recharge occurs seasonally. The percentage of young water in the water of a well pumping from such a stratified reservoir depends on its distance to the exfiltration zone, its depth and the position and length of its screen. The pumping rate and the pump position also play a crucial role for the depth from which water is preferentially extracted (Houben and Hauschild

DOI 10.1007/s10040-014-1169-2

2011). Unfortunately, the well owners could provide almost none of this information, sometimes not even the well depth; therefore further interpretation is refrained from. Nevertheless, from the isotopic evidence, the following three key findings can be safely deduced:

1. Groundwater recharge is taking place.
2. The bulk of the water presently found in the freshwater lens predates the atmospheric atomic bomb tests.
3. Water in the deeper part of the lens may be up to a thousand or more years old.

The Rio Verde showed a tritium concentration of 3.3 TU in 2009, very similar to recent rainfalls, which is another indication that it is almost entirely rainfed and neither receives nor infiltrates significant volumes of water from or to the freshwater lens.

Water balance

More than 95 % of the population of Benjamín Aceval and Cerrito are connected to one of the four public (Junta de Saneamiento) or the one private water supply companies, each operating one to five wells. According to the Paraguayan census, confirmed by our own local survey (sample of 278 households), one household (= connection) equals five persons. The 650 clients of the private company have household water meters and pay for the volume used. The company provided us with their sales figures for 2008, separated for household and business clients. Including small businesses like shops, bakeries and butchers, the daily per capita net water consumption is 88 l/day·person. Small businesses excluded, household water consumption is only 55 l/day·person. It has to be taken into account that the standard of living is usually quite humble. Only about half of all households have washing machines and three quarters have bathrooms with running water. We were also able to compare sold water to the volume pumped from the wells. Discounting illegal and thus unpaid connections, gross water consumption is 120 l/day·person. Net losses through leaky pipelines must therefore be in the range of 25 % of pumped water.

Clients of the public waterworks pay a monthly flat charge. Water meters were installed on all wells to monitor the volume of abstracted water for 1 year at a monthly interval. Table 1 summarizes the results of water consumption. Some of the other, smaller settlements have their own water supply for which data mostly had to be estimated; however, their contribution is relatively small.

Three agroindustrial enterprises also extract freshwater from their own wells; although, unfortunately, no data on abstraction volumes were available. The first, a sugar cane factory, produces 7,000 t of sugar per year from 75,000 t of sugar cane. They estimate a water consumption of 10 m^3 per ton of sugar, which equals 70,000 m^3/year. The factory has one active well but also uses water from rainwater storage ponds. The second user, a chicken farm, raises 360,000 animals per year. According to the owners, a chicken requires 0.3 l/day, which equals 39,500 m^3/year, all taken from two wells. The water-intensive processing of animal meat is done outside the catchment. For the third user, a small factory that produces alcohol from sugar cane, a water consumption of≈10,000 m^3/year, all groundwater, was estimated. Total industrial abstraction should be around 120,000 m^3/year. Total groundwater extraction from the freshwater lens should, thus, amount to 855,000 m^3/year. The total number of persons calculated in Table 1 coincides very well with population numbers from the national census, which shows that our calculations are comprehensive.

Table 2 summarizes the volume of groundwater recharge at different recharge rates for the big freshwater lens from which most of the inhabitants (estimate: 16,000) are supplied with water. In a drier year with only 2.5 % of rainfall being recharged (35 mm/year), the recharged volume practically balances the water consumption. In wetter years, the situation becomes less critical. In general, groundwater extraction is, therefore, sustainable at the moment, which might change if the population increases significantly, especially due to relocations from overcrowded Greater Asunción, and if more water-intensive industries would be installed. The limitations of the water resources therefore impose constraints on the future development of the city. No reliable data on the volume of re-infiltrated wastewater are available but the abundance of faecal bacteria shows that it must be significant (see the following). If the city would install a central wastewater recollection and a system to overcome the pollution of its central water resource, this could, ironically, tip the water balance towards over-exploitation in dry years, if the treated water is not re-infiltrated.

The surface area of the freshwater lenses is about 24.5 km^2. Assuming an average thickness of 80 m and a porosity of 10 %, the static freshwater water volume would be 196 million m^3. A recharge of 80 mm/year, thus, corresponds to 1 % of the total volume, making the turnover time around 100 years.

Water quality

Samples were taken from all 38 available deep wells and from one spring. All groundwater samples are of the $NaHCO_3$ type. In contrast, eight rainwater samples collected in Asunción in the period from 2008 to 2010 all showed a $CaHCO_3$ type, indicating a continental origin. During infiltration, or within the aquifer, the water composition is obviously affected by cation exchange: calcium is absorbed and replaced by sodium. The abundance of sodium can only mean that

DOI 10.1007/s10040-014-1169-2

Table 1 Water abstraction for public water supply from the freshwater lens (based on data from 2008 and 2009)

Water supplier	No. of wells	Pumped volume [m^3/year]	Connections [No. of households]	Clients [No. of persons]	Daily gross consumption [l/day·person]
JdS B. Aceval	3	305,300	1,220	6,100	111
JdS Cerrito	5	210,400	770	3,850	135
JdS Isla Ita	1	31,800	135	675	115
JdS Costa Guazu	1	23,500	100	500	115
Private water work	2	103,300	648	3,240	120
Military housing	1	4,000[a]	16	80	135[a]
Barracks	1	4,500[a]	–	125	100[a]
Worker settlement	1	8,800[a]	42	210	120[a]
Agricultural school	2	15,500[a]	–	170	250[a]
Toba Qom (indigenous)	1	28,500[a]	?	1,300	60[a]
SUM public	18	735,600	–	16,250	–

[a] Estimated

the aquifer was once completely filled with saline water, as is present in the Chaco lowland, which saturated the exchange sites with sodium. The cumulative amount of calcium introduced by fresh groundwater recharge in the last centuries or even millennia has not yet been sufficient to eliminate the sorbed sodium. To test this hypothesis, the Base Exchange Index (BEX) was calculated after Stuyfzand (2008) (Eq. 8).

$$BEX = [Na] + [K] + [Mg] - 1.0716 \times [Cl] \quad (8)$$

where

[Na], [K], [Mg] and [Cl]	concentrations of these ions in mmol(eq)/L
1.0716	([Na]+[K]+[Mg])/[Cl] for seawater

A negative BEX shows an ongoing salinisation trend, a positive BEX indicates propagation of fresh water. Of the 38 groundwater samples, 33 showed a positive BEX, indicating ongoing freshening, which is consistent with the hypothesis of cation exchange influencing the water chemistry.

The lack of a sewage system is reflected by the spatially comprehensive abundance of faecal bacteria in groundwater samples (Fig. 13). Coliforms were found in 70 % of all samples and *E. coli* in 40 %. The negative effects of wastewater infiltration on the chemical composition of the groundwater, on the other hand, are rather small. Not one sample exceeds the Paraguayan maximum permissible value of 45 mg/l for nitrate. 80 % have concentrations below 10 mg/l and only one sample exceeds 20 mg/l. The simultaneous input of faecal matter, together with the elevated temperatures, obviously promotes heterotrophic denitrification which controls nitrate concentrations (Houben et al. 2009).

Three samples from private wells showed fluorine concentrations surpassing the Paraguayan maximum permissible value of 1.5 mg/l, two of which originated from wells pumping water of elevated salinity which precludes their use. Conversely, the river water of the Rio Verde differs strongly from the composition of groundwater. It shows significant amounts of dissolved humic acids (30 % of the molar equivalent anion balance), giving it a distinct colour which cannot be removed by filtration. As groundwater from the freshwater lens does not show this feature, this is another indicator that the Rio Verde and the freshwater lens hardly interact.

Table 2 Water balance for the main freshwater lens (16,000 users) at different recharge rates (area=24.5 km^2)

Recharge rate [mm/year]	Recharged volume [m^3/year]	Disposable volume [l/day·person]	Water balance (consumption 855,600 m^3/year) [m^3/year]
35	857,500	147	+ 1,900
70	1,715,000	294	+ 859,400
80	1,960,000	336	+ 1,104,400
140	3,434,000	588	+ 2,578,400

Conclusion and summary

The groundwater body found underneath the hills of Benjamín Aceval is an isolated freshwater lens in dynamic equilibrium with saline groundwater in the surrounding Chaco lowlands (Fig. 14). To the authors' knowledge, this is the first description of such a Ghyben-Herzberg lens far from the ocean. Both the analytical and numerical models indicate that the freshwater heads are strongly influenced by the presence of a low-permeability layer at around 100 m depth, which causes a strong increase of the fresh groundwater level above the saltwater level. Whether freshwater has penetrated further downwards could not be validated as no deep wells are

DOI 10.1007/s10040-014-1169-2

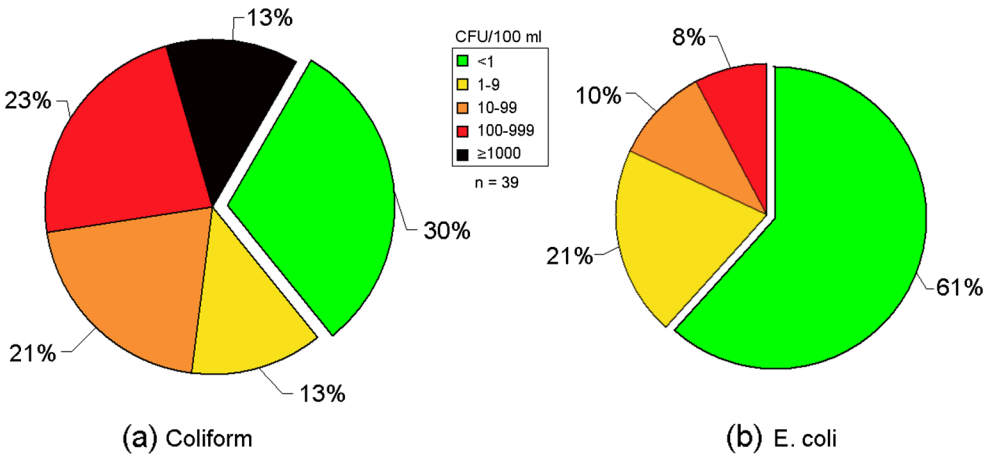

Fig. 13 Counts of indicator bacteria for faecal contamination in groundwater: **a** total coliforms, **b** *E. coli* (*CFU* = colony forming units)

available and the used geophysical measurements cannot penetrate through the basal layer.

The Rio Verde, despite its spatial proximity, does not play a role in the water balance of the freshwater lens, as water levels, tritium concentrations and hydrochemistry indicate. It only acts as a sink for some discharge from the eastern flank of the lens. The freshwater lens is, thus, a hydraulically independent water body, recharged only by infiltrating rainwater and sewage return flow.

The groundwater recharge rate ranges around 85 mm/year; however, a rate as low as 35 mm/year is sufficient to balance the current extraction of groundwater. Significant increases in extraction have to be avoided, though, especially in the light of potential climate change which might lead to a drier climate.

The bulk of the water presently found in the freshwater lens predates the atmospheric atomic bomb tests. Water in the deeper part of the lens may be up to a thousand or more years old. Return flow from numerous cesspits and latrines must be taken into account as additional groundwater recharge, yet has seriously deteriorated water quality, especially by faecal bacteria, which can only be overcome by a future wastewater collection, treatment and reinfiltration system.

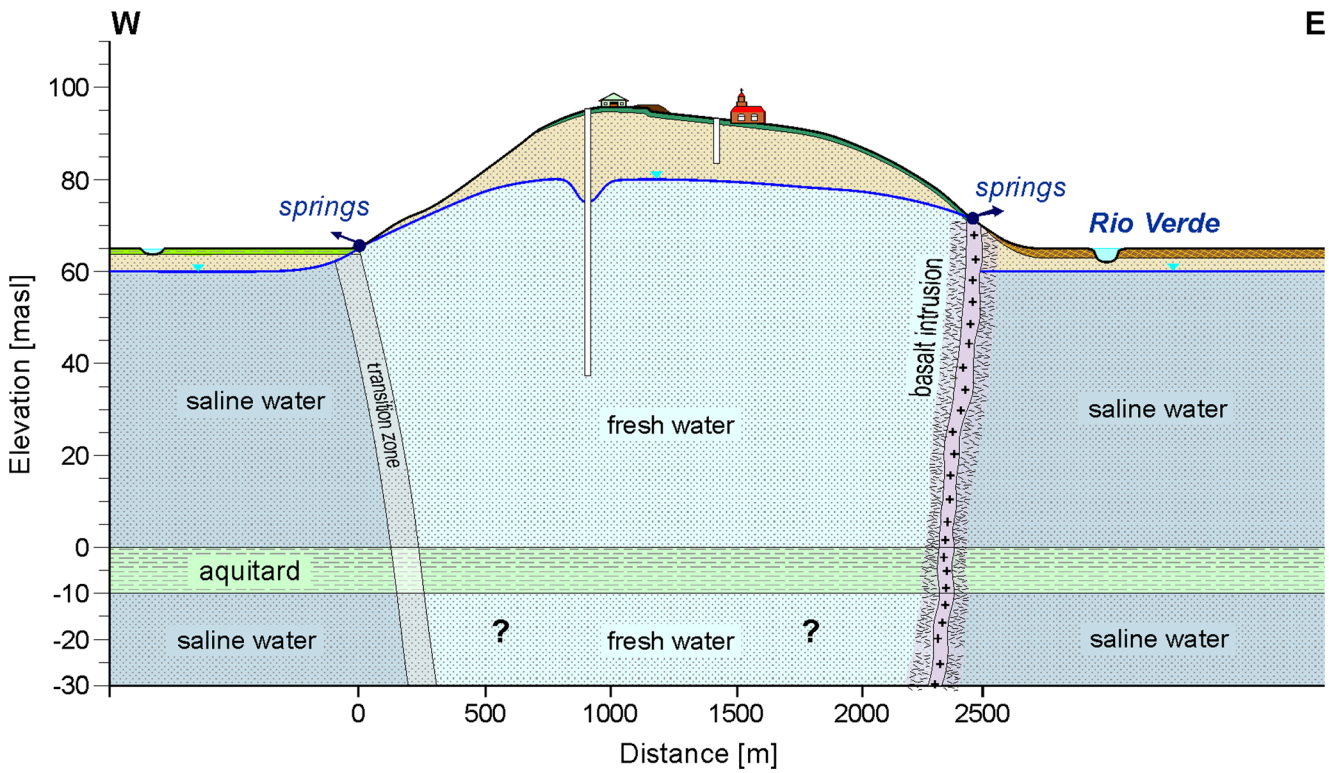

Fig. 14 Conceptual model sketch of the Benjamín Aceval freshwater lens

DOI 10.1007/s10040-014-1169-2

Acknowledgements This study was funded by the German Federal Ministry of Economic Cooperation and Development (BMZ) within the Paraguayan-German Project 2004.2189, carried out jointly by the Secretaria del Medio Ambiente (SEAM), Paraguay, and the Federal Institute of Geosciences and Natural Resources (BGR), Germany.

References

Ayers JF, Vacher HL (1986) Hydrogeology of an atoll island: a conceptual model from detailed study of a Micronesian example. Ground Water 24(2):185–198

Bailey RT, Jenson JW, Olsen AE (2009) Numerical modeling of atoll island hydrogeology. Ground Water 47(2):184–196

Barrett B, Heinson G, Hatch M, Telfer A (2002) Geophysical methods in saline groundwater studies: locating perched water tables and fresh-water lenses. Explor Geophys 33(2):115–121

Batu V (1998) Aquifer hydraulics: a comprehensive guide to hydrogeologic data analysis. Wiley, New York, 752 pp

Baydon-Ghyben W (1898) Nota in verband met de voorgenomen putboring nabij Amsterdam [Note concerning the water well drilled near Amsterdam]. Koninglijk Instit Ing Tijdschrift 1888–89:8–22

Bear J, Cheng A-HD, Sorek D, Ouazar DS, Herrera I (2010) Seawater intrusion in coastal aquifers concepts, methods and practices. Springer, Berlin, 625 pp

Bitschene PR (1987) Mesozoischer und känozoischer anorogener Magmatismus in Ostparaguay: Arbeiten zur Geologie und Petrologie zweier Alkaliprovinzen [Mesozoic and Cenozoic anorogenic magmatism in eastern Paraguay: studies of geology and petrology of two alkaline provinces]. PhD Thesis, Heidelberg University, Germany]

Bitschene PR, Báez Presser JL (1989) The Asunción Alkaline Province (eastern Paraguay): geologic setting and petrogenetic aspects. Zentralbl Geol Paläontol 1(5–7):959–971

Cartwright I, Weaver TR, Simmons CT, Fifield LK, Lawrence CR, Chisari R, Varley S (2010) Physical hydrogeology and environmental isotopes to constrain the age, origins, and stability of a low-salinity groundwater lens formed by periodic river recharge: Murray Basin, Australia. J Hydrol 380:203–221

Chesnaux R, Allen DM (2008) Groundwater travel times for unconfined island aquifers bounded by freshwater or seawater. Hydrogeol J 16(3):437–445

Christiansen AV, Auken E (2012) A global measure for depth of investigation. Geophysics 77(4):WB171–WB177

Clarke WB, Jenkins WJ, Top Z (1976) Determination of tritium by mass spectrometric measurement of ^{3}He. Int J Appl Radiat Is 27(9):515–522

Comin-Chiaramonti P, Civetta L, Petrini R, Piccirillo EM, Bellieni G, Censi P, Bitschene P, Demarchi G, De Min A, de Barro GC, Castillo AM, Velazquez JC (1991) Tertiary nephelinitic magmatism in eastern Paraguay: petrology, Sr–Nd isotopes and genetic relationships with associated spinel-peridotite xenoliths. Eur J Mineral 3(3):507–525

Comin-Chiaramonti P, Cundari A, Piccirillo EM, Gomes CB, Castorina F, Censi P, De Min A, Marzoli A, Speziale S (1997) Potassic and sodic igneous rocks from eastern Paraguay: their origin from the lithospheric mantle and genetic relationships with the associated Parana flood tholeiites. J Petrol 38(4):495–528

Comin-Chiaramonti P, Cundari A, DeGraff JM, Gomes CB, Piccirillo EM (1999) Early cretaceous–Tertiary magmatism in eastern Paraguay (western Paraná Basin): geological, geophysical and geochemical relationships. J Geodyn 28:375–391

Comin-Chiaramonti P, Marzoli A, de Barros GC, Milan A, Riccomini C, Velazquez VF, Mantovani MMS, Renne P, Tassinari CCG, Vasconcelos PM (2007) The origin of post-Paleozoic magmatism in eastern Paraguay. Geol Soc Am Spec Pap 430:603–633

Cooper HH, Kohout FA, Henry HR, Glover RE (1964) Seawater in coastal aquifers. US Geol Surv Water Suppl Pap 1613-C:84

Cortelezzi CR, Colado UR, Muñoz L (1988) Disyunción columnar en areniscas mesozoicas (Formación Misiones), Republica del Paraguay [Columnar jointing in mesozoic sandstones (Misiones formation), Republic of Paraguay]. Notas Museo Del Plata Geol 76:169–175

Dose EJ, Stoeckl L, Houben GJ, Vacher L, Vassolo S, Dietrich J, Himmelsbach T (2014) Experiments and modeling of freshwater lenses in layered aquifers: steady state interface geometry. J Hydrol 509:621–630

EN ISO 748 (2007) Hydrometry: measurement of liquid flow in open channels using current-meters or floats. ISO, Geneva

Facetti-Fernandez JF, Stichler W (1995) Analysis of concentration of environmental isotopes in groundwater and rainwater from Paraguay. In: Proceedings of the Symposium on Isotopes in Water Resources Management, Vienna, March 1995, pp 439–444

Fetter CW (1972) Position of the saline water interface beneath oceanic islands. Water Resour Res 8(5):1307–1315

Geyh M, Grosjean M, Nunez LA, Schotterer U (1999) Radiocarbon reservoir effect and the timing of the late-glacial/early Holocene humid phase in the Atacama Desert, northern Chile. Quat Res 52:143–153

Greskowiak J, Röper T, Post VEA (2013) Closed-form approximations for two-dimensional groundwater age patterns in a fresh water lens. Ground Water 51(4):629–634

Grosjean M, Veit H (2005) Water resources in the arid mountains of the Atacama Desert (northern Chile): past climate changes and modern conflicts. In: Huber UM, Bugmann HKM, Reasoner M (eds) Global change and mountain regions: an overview of current knowledge. Springer, Dordrecht, The Netherlands, pp 93–104

Günther T (2004) Inversion methods and resolution analysis for the 2D/3D reconstruction of resistivity structures from DC measurements. PhD Thesis, Freiberg University, Germany

Herzberg A (1901) Die Wasserversorgung einiger Nordseebäder [The water supply of some North Sea baths]. J Gasbeleuchtung Wasserversorgung 44:815–819 (in German)

Houben G, Hauschild S (2011) Numerical modeling of the near-field hydraulics of water wells. Ground Water 49(4):570–575

Houben G, Tünnermeier T, Eqrar N, Himmelsbach T (2009) Hydrogeology of the Kabul basin (Afghanistan), part II: groundwater geochemistry. Hydrogeol J 17(4):935–948

Ivanov NN (1954) The determination of potential evapotranspiration (in Russian). Izvestiia Vsesojuszogo Geograficheskogo Obschetva, Ser. T, 86 (2), Izd-vo Akademii Nauk SSSR, Moscow

Kinzelbach W, Aeschbach W, Alberich C, Goni IB, Beyerle U, Brunner P, Chiang W-H, Rueedi J, Zoellmann K (2002) A survey of methods for groundwater recharge in arid and semi-arid regions. Early Warning and Assessment Report Series, UNEP/DEWA/RS.02-2. United Nations Environment Programme, Nairobi, Kenya

Langevin CD, Guo W (2006) MODFLOW/MT3DMS-based simulation of variable density ground water flow and transport. Ground Water 44(3):339–351

McClain ME (ed.) (2002) The ecohydrology of South American rivers and wetlands. IAHS Spec. Publ. 6, IAHS, Wallingford, UK, 215 pp

Riccomini C, Fernandez Velázquez V, de Barros GC (2001) Cenozoic lithospheric faulting in the Asunción rift, eastern Paraguay. J South Amer Earth Sci 14(6):625–630

Spitz K, Moreno J (1996) A practical guide to groundwater and solute transport modelling. Wiley, New York, 461 pp

Stoeckl L, Houben G (2012) Flow dynamics and age stratification of freshwater lenses: experiments and modeling. J Hydrol 458–459:9–15

Stuyfzand PJ (2008) Base exchange indices as indicators of salinization or freshening of (coastal) aquifers. In: Proceedings of the 20th Salt Water Intrusion Meeting, Naples, FL, USA, June 2008, pp 262–265

Sültenfuß J, Roether W, Rhein M (2009) The Bremen mass spectrometric facility for the measurement of helium isotopes,

neon, and tritium in water. Isot Environ Health Stud 45(2):83–95
Vacher HL (1988) Dupuit-Ghyben-Herzberg analysis of strip-island lenses. Geol Soc Amer Bull 100:580–591
Veit H (1995) Jungquartäre Landschaft- und Klimaentwicklung der zentralen Anden und ihres westlichen Vorlandes: Kenntnisstand und Probleme [Upper Quaternary landscape and climate evolution of the central Andes and their western foreland: state of research and problems]. Geomethodica 20:163–194
Velazquez VF, Comin-Chiaramonti P, Cundari A, de Barros GC, Riccomini C (2006) Cretaceous Na-alkaline magmatism from the Misiones Province (Paraguay): its relationships with the Paleocene Na-alkaline analog from Asunción and geodynamic significance. J Geol 114(5):593–614
Velázquez VF, Fonseca Giannini PC, Riccomini C, Martins Sallun AE, Hachiro J, de Barros GC (2008) Columnar joints in the Patiño formation sandstones, eastern Paraguay: a dynamic interaction between dyke intrusion, quartz dissolution and cooling-induced fractures. Episodes J Int Geosci 31(3):302–308
Vogel JC (1967) Investigation of groundwater flow with radiocarbon. Proc. series, IAEA, Geneva, pp 355–368
Vogel JC (1970) Carbon-14 dating of groundwater. Proc. series, IAEA, Geneva, pp 225–239
Werner AD, Bakker M, Post VEA, Vandenbohede A, Lu C, Ataie-Ahstiani B, Simmons CT, Barry DA (2012) Seawater intrusion processes, investigation and management: recent advances and future challenges. Adv Water Resour 51:3–26

 DOI 10.1007/s10040-014-1169-2